2022-01-0736 Published 29 Mar 2022



Rule-Based Power Management Strategy of Electric-Hydraulic Hybrid Vehicles: Case Study of a Class 8 Heavy-Duty Truck

Yongsoon Yoon Oakland University

Giovanni Romero New Jersey Institute of Technology

Emil Nkemdilim-Dantzler University of Michigan

Dan DelVescovo and Laila Guessous Oakland University

Citation: Yoon, Y., Romero, G., Nkemdilim-Dantzler, E., DelVescovo, D. et al., "Rule-Based Power Management Strategy of Electric-Hydraulic Hybrid Vehicles: Case Study of a Class 8 Heavy-Duty Truck," SAE Technical Paper 2022-01-0736, 2022, doi:10.4271/2022-01-0736.

Received: 07 Jan 2022 Revised: 07 Jan 2022 Accepted: 06 Jan 2022

Abstract

obility in the automotive and transportation sectors has been experiencing a period of unprecedented evolution. A growing need for efficient, clean and safe mobility has increased momentum toward sustainable technologies in these sectors. Toward this end, battery electric vehicles have drawn keen interest and their market share is expected to grow significantly in the coming years, especially in light-duty applications such as passenger cars. Although the battery electric vehicles feature high performance and zero tailpipe emission characteristics, economic and technical issues such as battery cost, driving range, recharging time and infrastructure remain main hurdles that need to be fully addressed. In particular, the low power density of the battery limits its broad adoption in heavy-duty applications such as class 8 semi-trailer trucks due to the required size and weight of the battery and electric motor. Motivated by the high power density, low cost and potential for improving energy efficiency through regenerative braking of a hydraulic pump and accumulator, this work numerically investigates the application

of an electric-hydraulic hybrid powertrain to heavy-duty class 8 semi-trailer trucks. A simulation model which includes an electric motor/generator, lithium-ion battery, hydraulic pump/ motor and hydraulic accumulator is developed. Using the simulation model, a rule-based power management strategy is developed to benefit from the different characteristics of the electric and hydraulic power sources and demonstrated with the numerical simulation of different driving cycles. The simulation results reveal that hybridization with the hydraulic pump/motor and accumulator can improve overall electric energy conversion efficiency by operating the electric motor in high energy efficiency zones, storing kinetic energy during deceleration using hydraulic regenerative braking, and reusing the regenerated energy during heavy acceleration at low speed. In addition, the peak electric power and total electric energy consumption are significantly reduced. Such reduced electric stress offers significant benefits including lower vehicle cost by reducing battery capacity and longer battery service life by reducing cyclic charging and discharging of the battery.

Introduction

ver the past several years, because of the increasing demand for net-zero emission economy, the automotive and transportation sectors have been dramatically changing with a major shift toward powertrain electrification. The market that had been dominated by internal combustion engines over the past century has been moving toward battery electric vehicles (BEV) or fuel cell electric vehicles (FCEV). This technical trend is particularly pronounced in light-duty applications such as passenger cars. On the other hand, widespread adoption of electrified powertrains in heavy-duty applications such as semi-trailer

trucks and vocational trucks has been limited by critical economic and technical limitations including battery cost, driving range, recharging time and infrastructure. Therefore, the heavy-duty applications where internal combustion engines dominate, continue to play a central role in contributing to global air pollution and greenhouse gas emissions.

Since the early 2000s, thanks to the high power density of a hydraulic pump/motor and accumulator, many studies have sought to combine hydraulic systems with internal combustion engines in, so called hydraulic hybrid vehicles (HHVs). The HHVs employ the internal combustion engine as a primary power source, and the hydraulic motor as a

secondary power source such as a hydraulic power assistance system that benefits from efficient hydraulic regenerative braking. Different architectures including series and parallel HHVs have been investigated and different design technologies have been developed [1-7]. Several works have looked at the application of rule-based and dynamic programming-based power management strategies to light/medium trucks or commercial heavy vehicles [1-4]. The last mile delivery van was developed to fully benefit from hydraulic regenerative braking from frequent stop-and-go [5]. Further studies include an online optimal power management using a model predictive control approach [6] and comparative studies on design and power management strategies [7].

Since the 2010s, electric components have replaced internal combustion engines in, so called electric-hydraulic hybrid vehicles (EH2Vs), due to the remarkable advancement of electrified powertrain technologies and stringent emission standards. Similarly, rule-based and optimal power management strategies have been developed with application to small trucks or city buses [8-16].

In this work, to promote broader adoption of electrified powertrains in heavy-duty applications, the EH2 powertrain is considered. Toward this end, this work numerically investigates the application of the EH2 powertrain to class 8 semitrailer trucks. The simulation model, including the electric powertrain (electric motor/generator and battery) and hydraulic powertrain (hydraulic pump/motor and accumulator) is developed in the MATLAB/Simulink environment based on physics and look-up tables for efficient and reliable simulation studies. Then, a rule-based power management strategy is developed and validated through simulation of different transient driving cycles.

The remainder of this paper is outlined as follows: Technical background including the hybrid powertrain configuration and backward simulation framework will be introduced in the following section. Next, the physics-based and lookup tables-based models of the electro-hydraulic hybrid (EH2) powertrain components are discussed. Then, the rule-based power management strategy design and its numerical validation will follow. Different driving cycles are simulated to illustrate the effectiveness of the proposed strategy. Finally, concluding remarks are provided.

Background

The configuration of the EH2 powertrain considered in this work is shown in Fig. 1. It consists of two different powertrain systems in parallel connection: electric and hydraulic systems. The electric powertrain includes the electric motor/generator (EMG) and battery as a power system and energy storage system, respectively. On the other hand, the hydraulic powertrain includes the hydraulic pump/motor (HPM) and accumulator as a power system and energy storage system, respectively. If the hydraulic components are removed, it is the same configuration of pure BEVs. The objective of this study is to use the EMG and battery in an efficient way by optimally distributing the power request to two different power and energy sources.

FIGURE 1 Configuration of the EH2 powertrain.

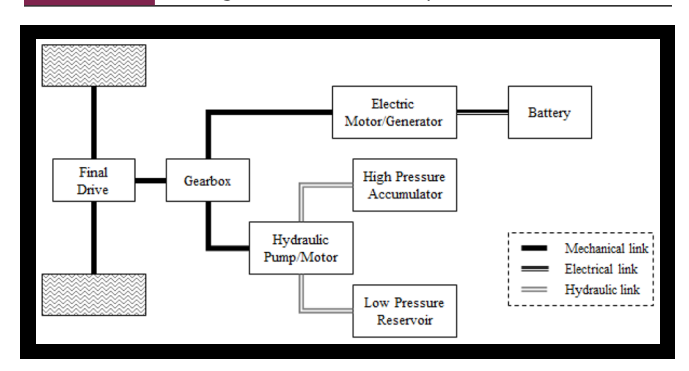
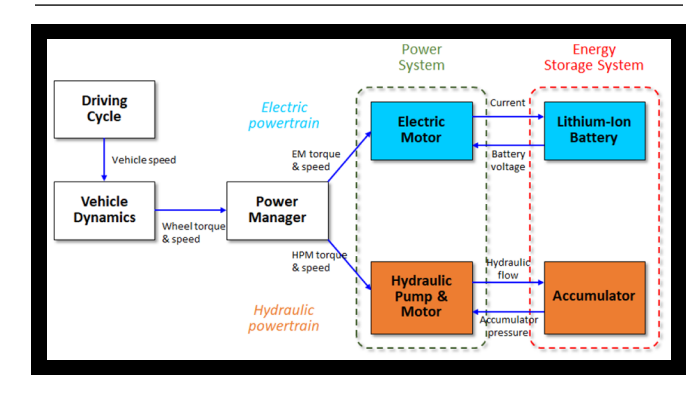


FIGURE 2 Signal flows in the backward simulation framework.



In this work, the rule-based power management strategy will be validated in a backward simulation framework due to its computational efficiency [9-12, 14, 16]. In a forward simulation framework, the states and control inputs of both powertrains determine the actual power, and in turn the generated power determines the vehicle speed depending on vehicle dynamics just like a real system. On the other hand, in the backward simulation framework, assuming a known driving cycle, the required power demand is calculated, then the states of both powertrains are analyzed when the proposed power management strategy is applied. The signal flows in the backward simulation framework are shown in Fig. 2.

EH2V Modeling

In this section, the simulation model of the electric-hydraulic hybrid vehicle (EH2V) (i.e. the input and output signals shown in Fig. 2) based on physics and look-up tables are presented in the order of the signal flows in the backward simulation framework. The relevant model parameters are obtained from the literature [16, 17] and MATLAB/Simulink Library [18] and rescaled for application to a heavy-duty class 8 truck. The model itself may lack high fidelity, however, it still can capture critical phenomena such as energy flow among different components. Hence, the reliability of the model will be sufficient in this case study that investigates the benefits of the proposed hybrid powertrain and power management strategy in terms of overall energy consumption and efficiency.

Driving Cycle

In this work, three different driving cycles including the Heavy-Duty Urban Dynamometer Driving Schedule (HDUDDS), Heavy Heavy-Duty Diesel Truck (HHDDT) transient mode and West Virginia University 5 Peak Cycle (WVU5PEAK) shown in Fig. 3 are considered. The HDUDDS was developed for a chassis dynamometer test of heavy-duty vehicles by the Environmental Protection Agency (EPA). It is 1060 seconds long, the total driving distance is 8.9 km and the average and maximum speed are 30.4 and 93.3 km/h, respectively. The HHDDT was developed for a chassis dynamometer test of heavy-duty vehicles by the California Air Resource Board (CARB) with the cooperation of West Virginia University. It is 668 seconds long, the total driving distance is 4.6 km and the average and maximum speed are 24.7 and 76.4 km/h, respectively. These two driving cycles emulate realword transient conditions and they have been broadly used to demonstrate transient capability of heavy-duty vehicles. The WVU5PEAK cycle was developed for a general truck chassis test by the Vehicle Emissions Testing Lab at West Virginia University. This cycle consists of five segments, each with an ideal acceleration, cruise and deceleration modes. It is 900 seconds long, the total driving distance is 8.05 km and it consists of five peak speeds at 32, 40, 48, 56 and 64 km/h.

Longitudinal Vehicle Model

<u>Fig. 4</u> illustrates the longitudinal dynamics of a semi-trailer truck. F_d , F_p , F_g and F_t are the air drag force, tire rolling resistance, projected weight onto the sloped road and traction force, respectively. ν and W are the longitudinal velocity and weight of the truck. The model parameters are based on the reference vehicle (FREIGHTLINER: eCascadia) as shown in Table 1.

Provided the vehicle speed profile is available from known driving cycles, the required tractive force for the truck to follow the speed is given by

$$F_t(t) = m\frac{dv}{dt} + F_r(t) + F_d(t) + F_g(t)$$
 (1)

The last three terms in the right-hand side are given by

$$F_r(t) = \mu_r mg \tag{2}$$

$$F_d(t) = \frac{1}{2} C_d \rho A_f \nu(t)^2 \tag{3}$$

$$F_{g}(t) = mg\sin\theta(t) \tag{4}$$

Then, the required wheel torque and corresponding wheel angular speed are given by

$$T_{w}(t) = F_{t}(t) \cdot R_{w} \tag{5}$$

$$\omega_w(t) = v(t) / R_w \tag{6}$$

The longitudinal dynamics given by (1) may include uncertainties, such as the unknown truck mass depending on passengers and cargo weight, rolling resistance coefficient

FIGURE 3 Heavy-Duty Urban Dynamometer Driving Schedule (top); Heavy Heavy-Duty Diesel Truck transient mode (middle); West Virginia University 5-Peak Cycle (bottom).

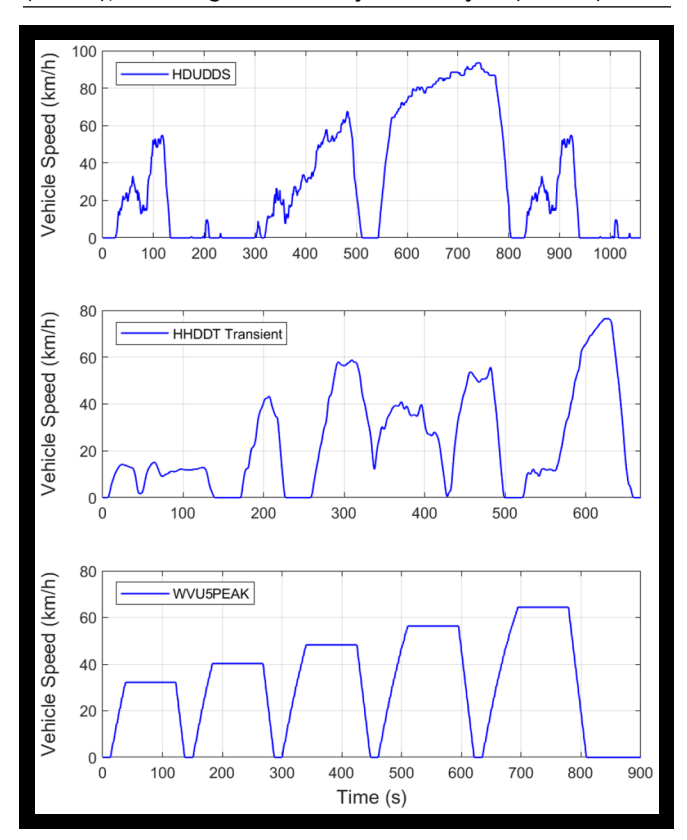


FIGURE 4 Longitudinal dynamics of a semi-trailer truck.

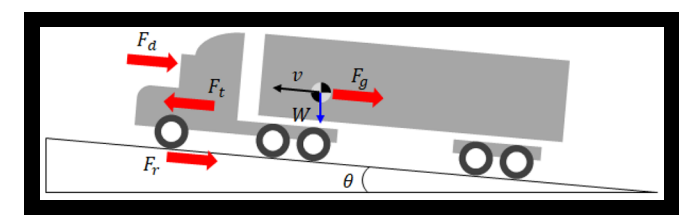


TABLE 1 Longitudinal Vehicle Model Parameters.

Description	Symbol	Values
Vehicle mass	m	15875.733 (kg)
Frontal projected area	A_f	10.2259 (m ²)
Wheel radius	R_w	0.5582 (m)
Gear ratio	i	12.5 (-)
Air drag resistance coefficient	C_d	0.3 (-)
Rolling resistance coefficient	μ_r	0.018 (-)
Air density	ρ	1.225 (kg/m ³)
Gravitational constant	g	9.81 (m/s ²)
Road angle	θ	0 (rad)

depending on the tire pressure and road surface condition and unknown road angle. Also, interference with the yaw and rolling dynamics of the truck can degrade accuracy of the longitudinal dynamics. However, these uncertainties are not considered in this work for simplicity.

Electric Motor

A high-efficiency and high-performance AC induction motor is considered in this study. This work considers a single speed gear reduction (*i*) for simplicity in modeling and power management strategy design. But, it can be easily extended to a multi-speed gearbox with minor modifications. The angular speed, mechanical torque and power of the electric motor are given by (7)-(9), respectively.

$$\omega_{EMG}(t) = \omega_w(t) \cdot i \tag{7}$$

$$T_{EMG}(t) = T_w(t)/i$$
 (8)

$$P_{EMG}(t) = T_{EMG}(t)\omega_{EMG}(t)$$
(9)

Then, the electric power and corresponding load current of the battery pack are given by (10) and (11).

$$P_{E}(t) = P_{EMG}(t) / \eta_{EMG}^{z}(t)$$
 (10)

$$I_B(t) = P_E(t) / V_B(t)$$
(11)

where $\eta_{EMG}(t)$ is the EMG efficiency as shown in Fig. 5 [17] and z is 1 for a motor mode and -1 for a generator mode.

Lithium-Ion Battery

A simple internal resistance lithium-ion battery model depicted in Fig. 6 is used in this study.

 $V_{oc}(t)$ and $R_{int}(t)$ are the open-circuit voltage and internal resistance depending on the battery core temperature $\Theta_B(t)$ and battery state-of-charge $SOC_B(t)$ as given in (11) and (12). They are both implemented as a two-dimensional look-up table [18].

$$V_{oc}(t) = f(\Theta_B(t), SOC_B(t))$$
(11)

$$R_{\rm int}(t) = g(\Theta_B(t), SOC_B(t))$$
 (12)

Then, assuming identical battery cells in the battery pack, the cell terminal voltage, cell load current and battery pack voltage are given by (13), (14) and (15), respectively. N_p and N_s are the number of cells in parallel and series connection in the battery pack.

$$V_t(t) = V_{oc}(t) - I_C(t)R_{int}(t)$$
(13)

$$I_C(t) = I_B(t) / N_p \tag{14}$$

$$V_B(t) = V_t(t)N_s \tag{15}$$

The state-of-charge of the battery is given by

$$SOC_{B}(t) = SOC_{B}(0) - \frac{1}{Ah} \int_{0}^{t} I_{C}(\tau) d\tau$$
 (16)

where Ah is the battery capacity in ampere-hour.

FIGURE 5 AC induction motor efficiency map.

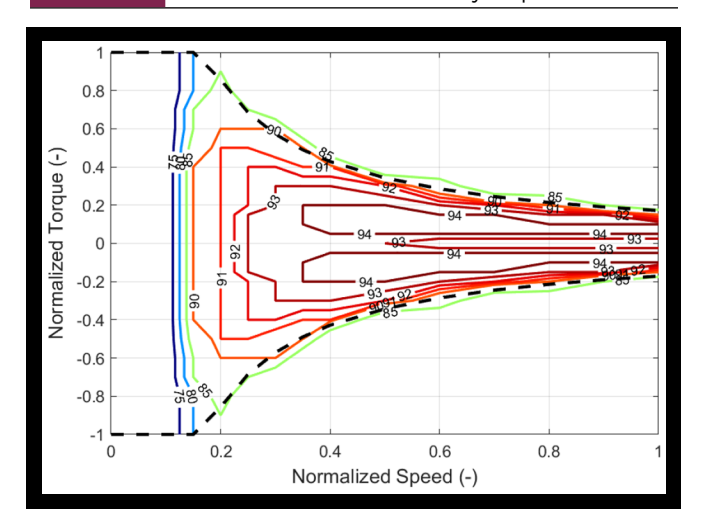
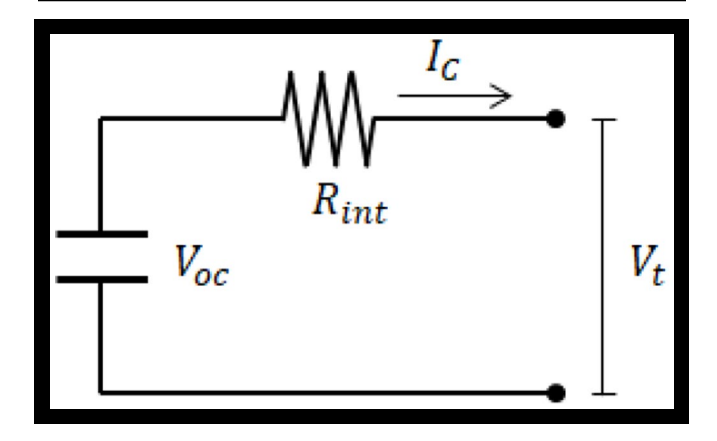


FIGURE 6 Lithium-ion battery circuit with internal resistance.



Variable Displacement Hydraulic Pump/Motor

A swashplate-type variable displacement hydraulic pump/motor [20] depicted in <u>Fig. 7</u> is considered for its high efficiency over the range of operating conditions. The hydraulic actuator controls the swashplate angle to achieve the variable oil displacement from/to the pistons.

The same gear ratio with the electric counterpart is considered for the HPM. The angular speed and mechanical torque and power of the HPM are given by

$$\omega_{HPM}(t) = \omega_{wh}(t) \cdot i \tag{17}$$

$$T_{HPM}(t) = T_{trac}(t) / i$$
 (18)

$$P_{HPM}(t) = T_{HPM}(t)\omega_{HPM}(t) \tag{19}$$

Then, the hydraulic torque and oil flow are obtained from

$$T_{H}(t) = (\alpha(t)D_{HPM})\Delta P_{accu}(t)\eta_{HPM}^{z}(t)$$
 (20)

$$q_{HPM}(t) = T_{trac}(\alpha(t)D_{HPM})\omega_{HPM}(t)\eta_{VEFF}^{-z}(t)$$
 (21)

where $\alpha(t)$ is the swashplate angle in radians and D_{HPM} is the maximum pump displacement in m³/radian, and z is 1 for

FIGURE 7 Schematic of a swashplate-type variable displacement hydraulic pump and motor.

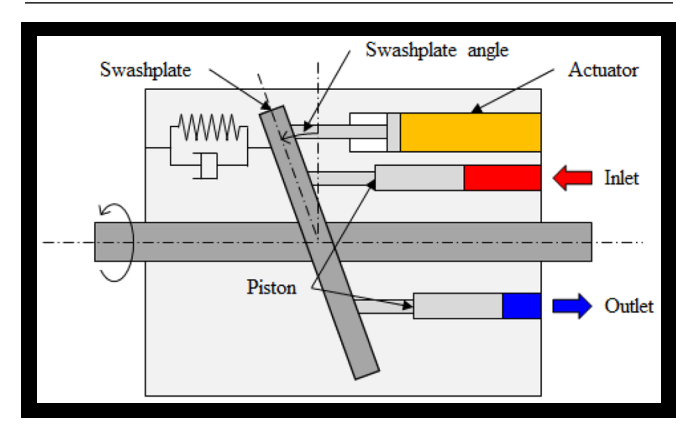
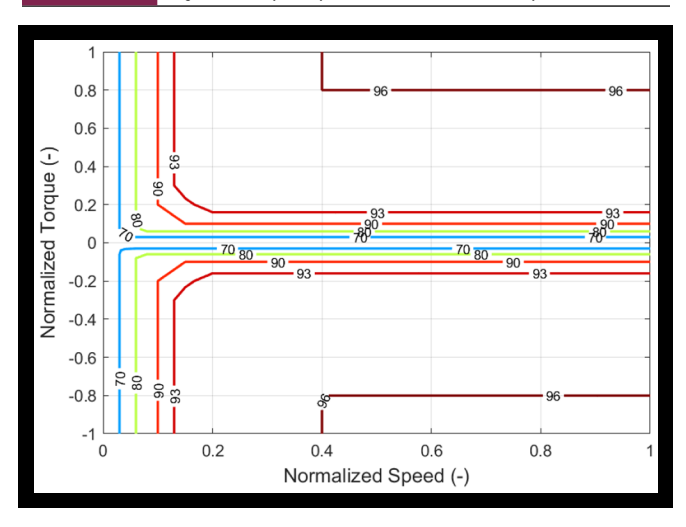


FIGURE 8 Hydraulic pump/motor efficient map.



a motor mode and -1 for a pump mode, respectively. $\eta_{HPM}(t)$ is the mechanical efficiency and $\eta_{VEFF}(t)$ is the volumetric efficiency. Fig. 8 shows the efficiency map of the hydraulic pump/motor [16].

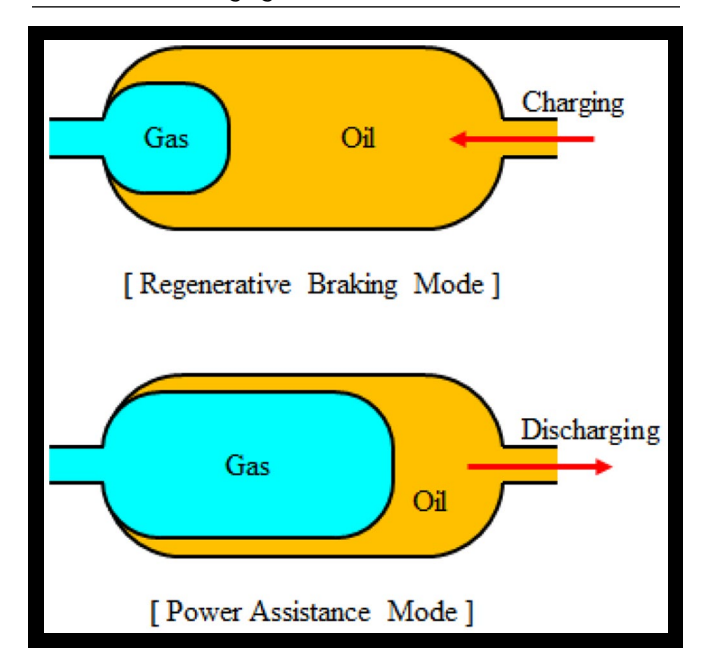
Accumulator

The EH2 powertrain needs an accumulator of high pressure and reservoir of low pressure. A bladder-type accumulator is used in this study for its high power density. Fig. 9. shows the high-pressure accumulator during a regenerative braking mode (upper) and power assistance mode (lower). During the hydraulic regenerative braking mode, the oil in the reservoir is pumped to the high-pressure accumulator and the kinetic energy is converted to hydraulic energy. During the power assistance mode, the oil in the high-pressure accumulator is discharged and the hydraulic energy is converted to kinetic energy.

Assuming adiabatic ($PV^n = constant$) and quasi-steady state process (i.e. gas pressure = oil pressure), the volumetric flow rate and pressure of the gas in the bladder are given by

$$\dot{V}_{gas}(t) = q_{HPM}(t) \tag{22}$$

FIGURE 9 Bladder-type accumulator: (upper) during a hydraulic regenerative braking mode \rightarrow oil charging from reservoir, (lower) during a hydraulic power assistance mode \rightarrow oil discharging to reservoir.



$$P_{gas}(t) = P_{pre} \left(\frac{V_{pre}}{V_{gas}(t)} \right)^{n}$$
 (23)

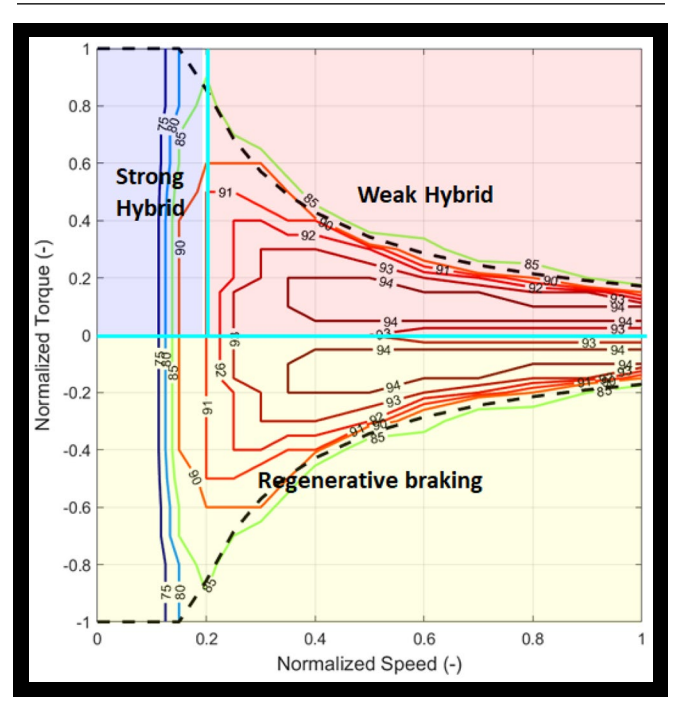
where P_{pre} and V_{pre} are the pre-charge pressure and volume to be determined and n=1.4 is the heat capacity ratio assuming an ideal gas. There exist different definitions of the state-of-charge of the accumulator in literature: 1) volume-based [1]; 2) pressure-based [6]; 3) energy-based [10]. In this study, the volume-based definition given by (24) is adopted for its computational simplicity.

$$SOC_{accu}(t) = \frac{V_{gas, max} - V_{gas}(t)}{V_{gas, max} - V_{gas, min}}$$
(24)

Rule-Based Power Management

In this section, the rule-based power management strategy is presented. As can be seen in <u>Fig. 10</u>, the fundamental limit of the electric motor is its low efficiency at low motor speed. If the normalized motor speed is less than 0.1, the efficiency becomes less than 75 %. Regarding this operating condition-dependent motor efficiency, three different modes are proposed.

For positive torque request, two hybrid propulsion modes are proposed. At low motor speed, where the electric motor efficiency is low, a high fraction of the propulsion **FIGURE 10** Power management strategy: different modes in the electric motor efficiency map space.



power comes from the hydraulic motor (i.e. a strong hybrid mode which means strong hydraulic power assistance). For example, a truck launch control or entering a highway may be in this mode. At high motor speed, where the electric motor efficiency is high, a low fraction of the propulsion power comes from the hydraulic motor (i.e. a weak hybrid mode). Highway cruising may be in this mode. These fractions depend on the state-of-charge of the accumulator and they are calibratable as shown in Fig. 11 since availability of the hydraulic power is limited by the state-of-charge of the high-pressure accumulator.

For negative torque request, the kinetic energy of the semi-trailer truck during deceleration can be converted into electric energy (electric regenerative braking) and/or hydraulic energy (hydraulic regenerative braking). In order to fully

FIGURE 11 Weak hybrid mode (low fraction of hydraulic power) and strong hybrid mode (high fraction of hydraulic power) depending on the state-of-charge of the accumulator.

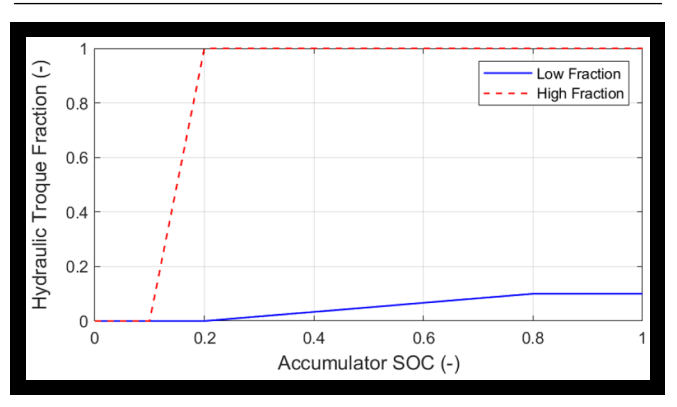


FIGURE 12 Rule-based power management strategy

```
If Torque Request > 0 (Propulsion Mode)
    If Speed > Threshold (EMG High Efficient Zone: Less Hydraulic Energy)
        HPM Torque Request = Torque Request x Low Fraction(Accumulator SOC)
    Else (EMG Low Efficient Zone: More Hydraulic Energy)
        HPM Torque Request = Torque Request x High Fraction(Accumulator SOC)
    EMG Torque Request = Torque Request - HPM Torque Request
    Mechanical Brake Torque = 0
Else (Brake Mode)
    If Accumulator SOC < Threshold (Hydraulic Regenerative Braking)
        HPM Torque Request = Low Band Torque Request
        EMG Torque Request = 0
        Mechanical Brake Torque = High Band Torque Request
        HPM Torque Request = 0
        If Battery SOC < Threshold (Electric Regenerative Braking)
             EMG Torque Request = Low Band Torque Request
            Mechanical Brake Torque Request = High Band Torque Request
        Else (Mechanical Braking)
            EMG Torque Request = 0
            Mechanical Brake Torque = Torque Request
    End
End
```

benefit from the high power density of the bladder-type accumulator and to reduce cyclic charge and recharge of the battery that may shorten the battery service time, the hydraulic regenerative braking takes higher priority. During the hydraulic regenerative braking mode, the oil in the reservoir is charged into the high-pressure accumulator until the state-of-charge of the accumulator hits the upper limit. Once it hits the limit, it turns to the electric regenerative braking until the state-of-charge of the battery reaches its maximum value.

Fig. 12 summarizes the proposed power management strategy. The necessary calibrations including the motor speed threshold and fractions of the hydraulic power should be determined based on driving cycle analysis. It is noted that during the brake mode, the hydraulic pump or electric generator will take the low pass filtered torque request and the mechanical brake (i.e. friction brake) will take the high pass filtered request to ensure accurate braking performance.

Simulation Results

The proposed rule-based power management strategy is validated in this section, and the benefits of the EH2 powertrain option for the heavy-duty truck are investigated. The specifications of the electric motor and battery are from the reference truck [21]: 1) Dual motor operating at 400 Volts: max wheel torque = 23,000 lb-ft (i.e. 31.2 kNm), max power = 360 hp (268.452 kW); 2) LiFePO4 battery: 475 kWh.

Fig. 13 shows the simulation results of the HDUDDS cycle with the EV (solid blue) and EH2V (dashed red) models. With the EH2 powertrain option, all of the kinetic energy during deceleration is converted to hydraulic energy through efficient hydraulic regenerative braking. By using this stored energy

FIGURE 13 HDUDDS Simulation: (1st row) vehicle speed, (2nd row) electric power; (3rd row) battery current; (4th row) battery SOC; (5th row) accumulator SOC.

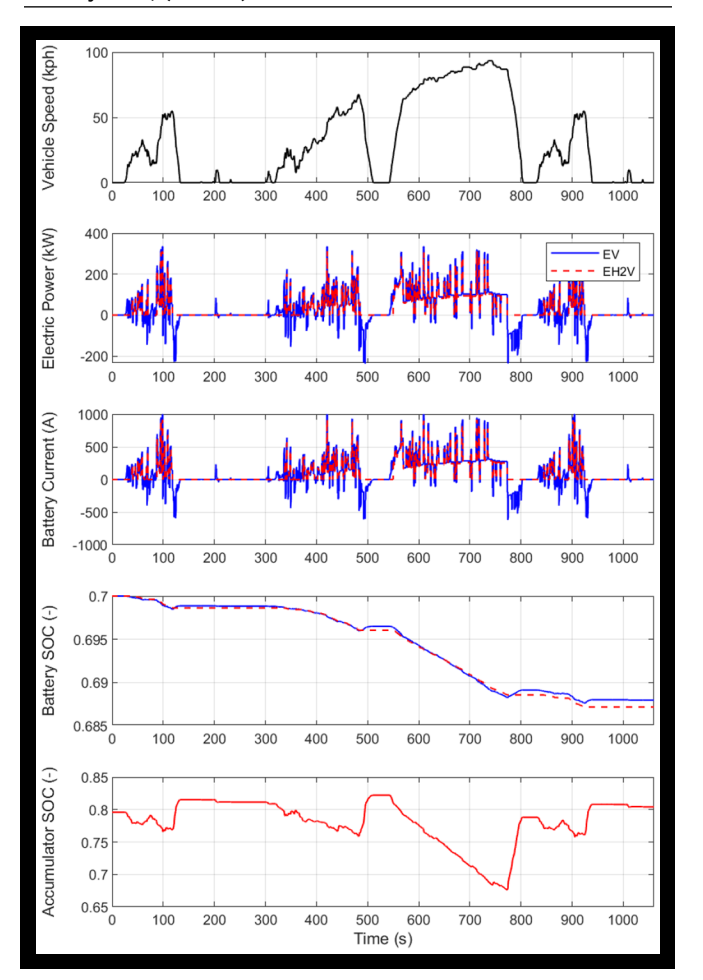
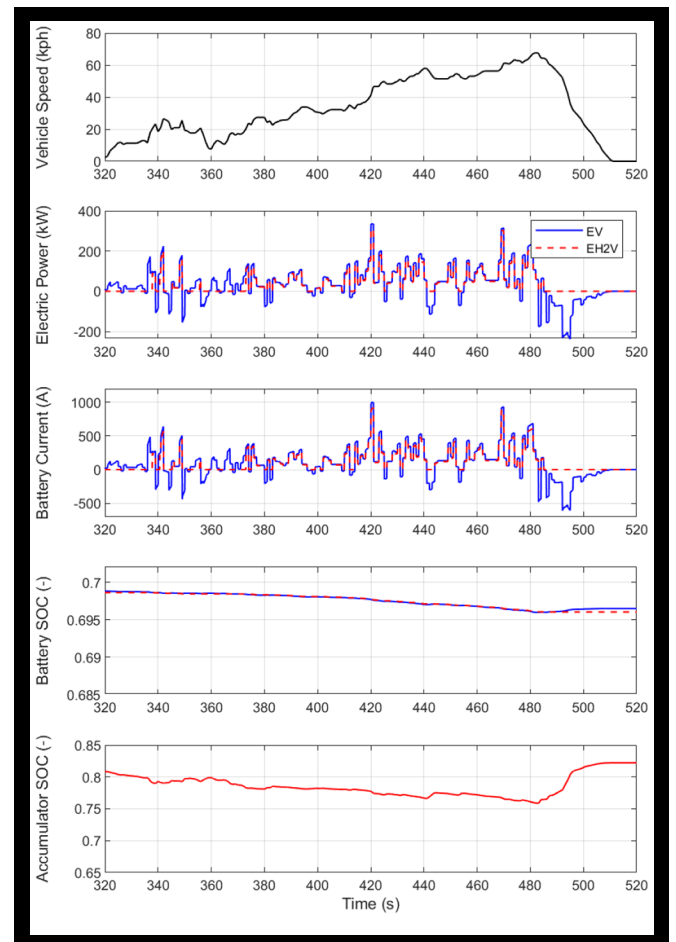


FIGURE 14 HDUDDS Simulation (zoom-in): (1st row) vehicle speed, (2nd row) electric power; (3rd row) battery current; (4th row) battery SOC; (5th row) accumulator SOC.



during heavy acceleration at low speed, the peak electric power and battery current load are reduced. The battery SOC is comparable even though electric regenerative braking is not used, which proves less electric energy from the battery was used during acceleration.

Fig. 14 is the close-up of the simulated HDUDDS cycle between 320 seconds and 520 seconds. This is a time period where the vehicle experiences slow acceleration followed by fast deceleration. Clearly, the electric power and battery current of the EH2V are lower during the first few seconds of heavy acceleration. The accumulator SOC of the EH2V recovers quickly during regenerative braking after 480 seconds.

As can be seen in <u>Fig. 15</u>, the EMG of the EH2V operates in the high energy efficiency zones (within the red contours), while that of the EV operates in the low energy efficiency zones during a significant period of time (in the blue contours).

Fig. 16 shows the simulation results of the HHDDT cycle with the EV (solid blue) and EH2V (dashed red) models. Similar results are observed. With the EH2 powertrain option, the kinetic energy is efficiently regenerated and by using this regenerated energy during acceleration at low speed, the electric stress is reduced.

FIGURE 15 HDUDDS Simulation: electric motor operation.

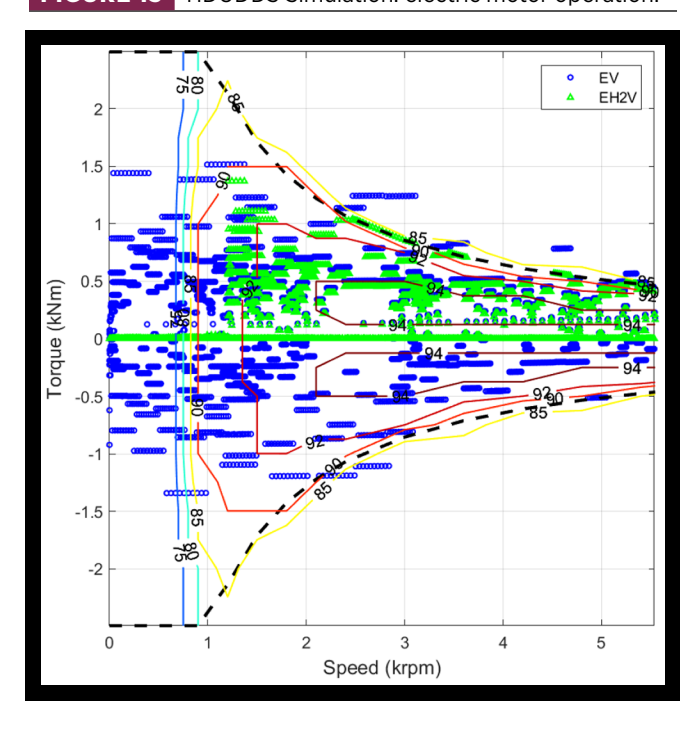


FIGURE 16 HHDDT Simulation: (1st row) vehicle speed, (2nd row) electric power; (3rd row) battery current; (4th row) battery SOC; (5th row) accumulator SOC.

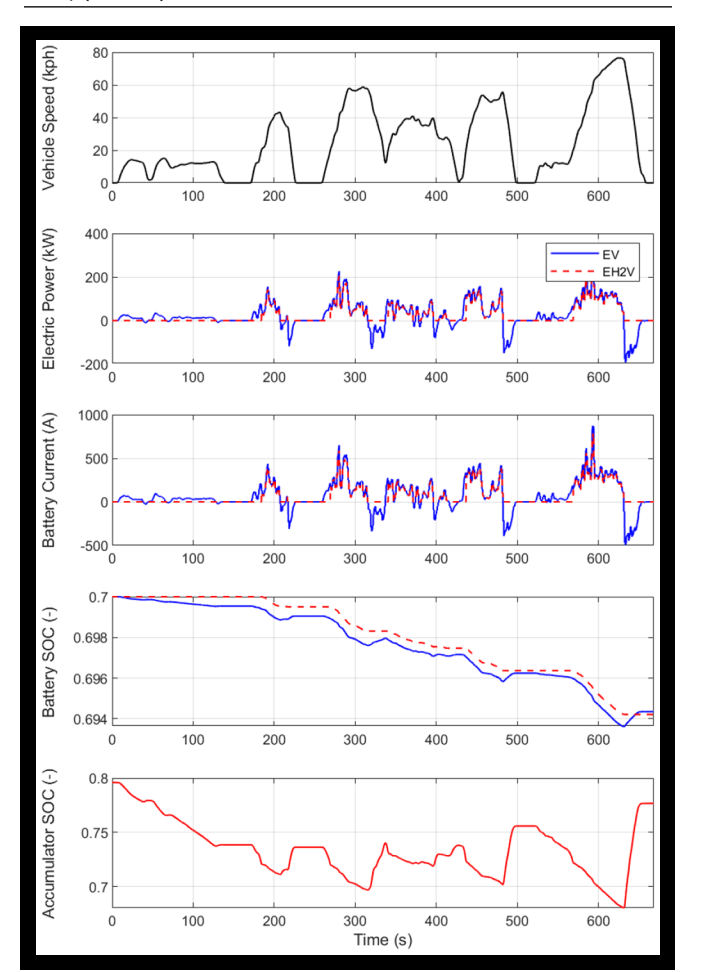


FIGURE 17 HHDDT Simulation (zoom-in): (1st row) vehicle speed, (2nd row) electric power; (3rd row) battery current; (4th row) battery SOC; (5th row) accumulator SOC.

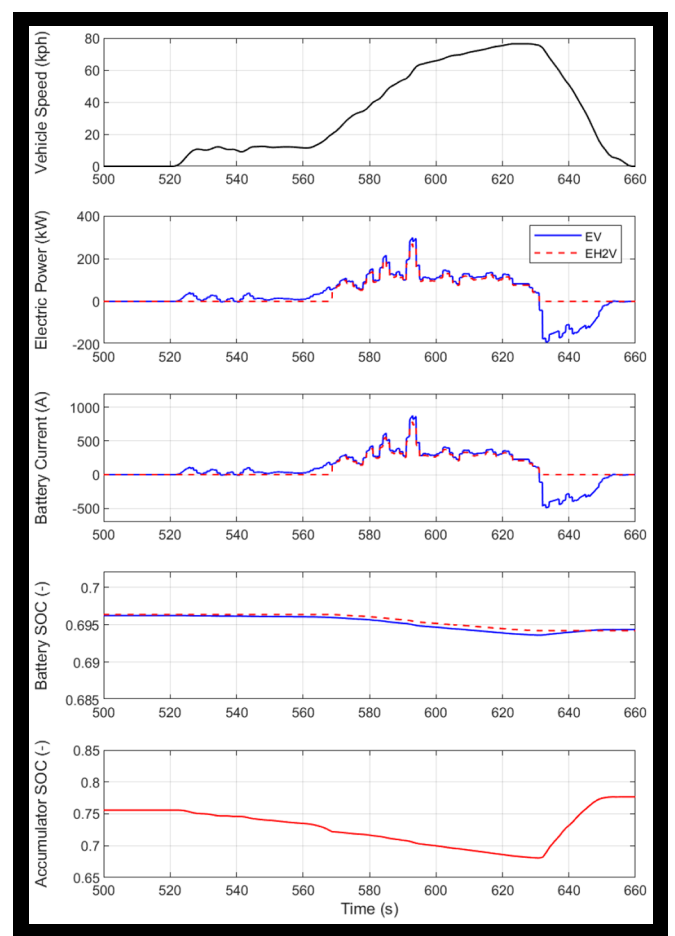


Fig. 17 is the close-up of the simulated HHDDT cycle between 500 seconds and 660 seconds. Similarly, the electric power and battery current of the EH2V are lower during heavy acceleration with the EH2 powertrain option. Additionally, the accumulator SOC of the EH2V recovers quickly during regenerative braking after 630 seconds.

Fig. 18 shows the EMG operation with the two different powertrain options. With the EH2 powertrain option, the EMG operates within the high energy efficiency zones, while the purely EV powertrain option results in inefficient operation of the EMG.

Fig. 19 shows the simulation results of the WVU5PEAK cycle with the EV (solid blue) and EH2V (dashed red) models. And Fig. 20 shows the zoom-in of Fig. 19 between 630 seconds and 850 seconds, i.e. the segment with the highest peak speed.

Fig. 21 shows the EMG operation during the cycle. Similarly, with the EH2 powertrain option, the hydraulic power assistance allows the EMG to operate in a more efficient way.

Fig. 22 shows the improvements of the EH2 powertrain option in terms of the total electric efficiency, peak battery power and total battery energy consumption over the EV

FIGURE 18 HHDDT Simulation: electric motor operation.

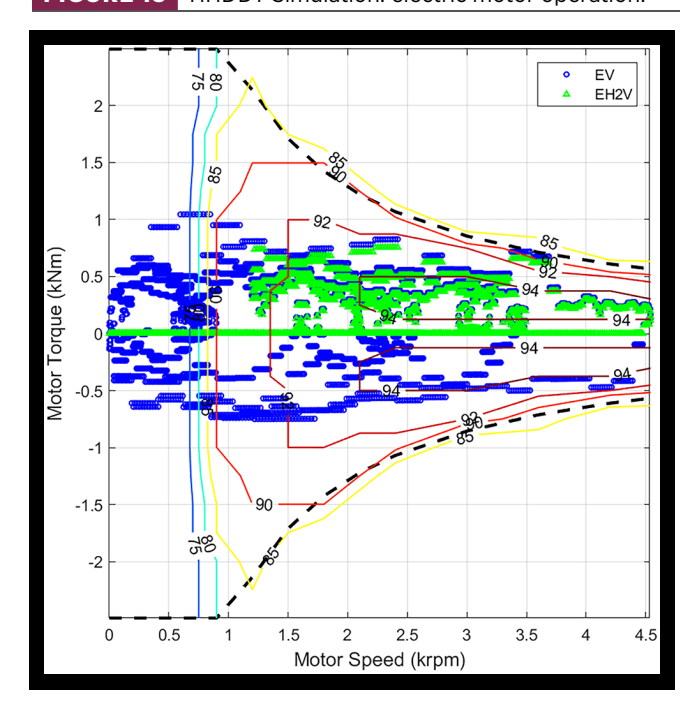
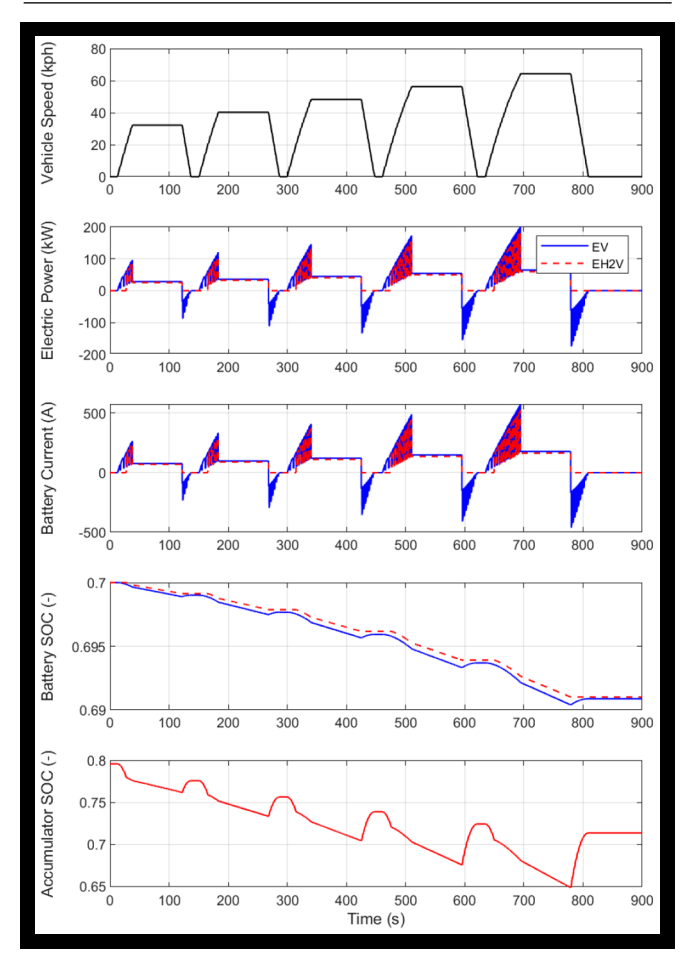


FIGURE 19 WVU5PEAK Simulation: (1st row) vehicle speed, (2nd row) electric power; (3rd row) battery current; (4th row) battery SOC; (5th row) accumulator SOC.



counterpart. The benefit with the EH2 powertrain option, to be specific the total battery energy consumption, is most significant under the HHDDT cycle since this cycle include a longer time period of heavy acceleration at low speed. But in all cases, the EH2 powertrain turns out to reduce electric stress, which means that vehicle cost can be lower by reducing the battery capacity and the battery service time can be extended by reducing cyclic charge and recharge of the battery.

Conclusions

In this work, the potential of an EH2 powertrain for a heavy-duty class 8 semi-trailer truck has been investigated. The backward simulation model that includes the electric and hydraulic power and energy storage systems has been developed in the MATLAB/Simulink environment. Based on the operational characteristics of the electric motor, a rule-based power management strategy is developed and demonstrated through numerical simulation of different driving cycles including HDUDDS, HHDDT and WVU5PEAK. The simulation results reveal that the overall electric energy conversion

FIGURE 20 WVU5PEAK Simulation (zoom-in): (1st row) vehicle speed, (2nd row) electric power; (3rd row) battery current; (4th row) battery SOC; (5th row) accumulator SOC.

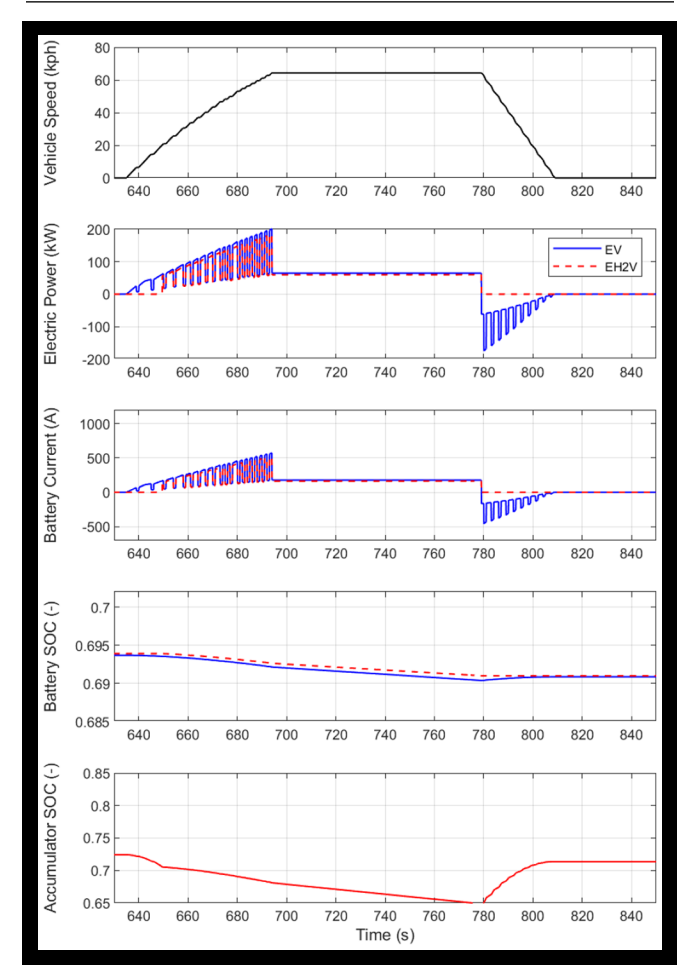
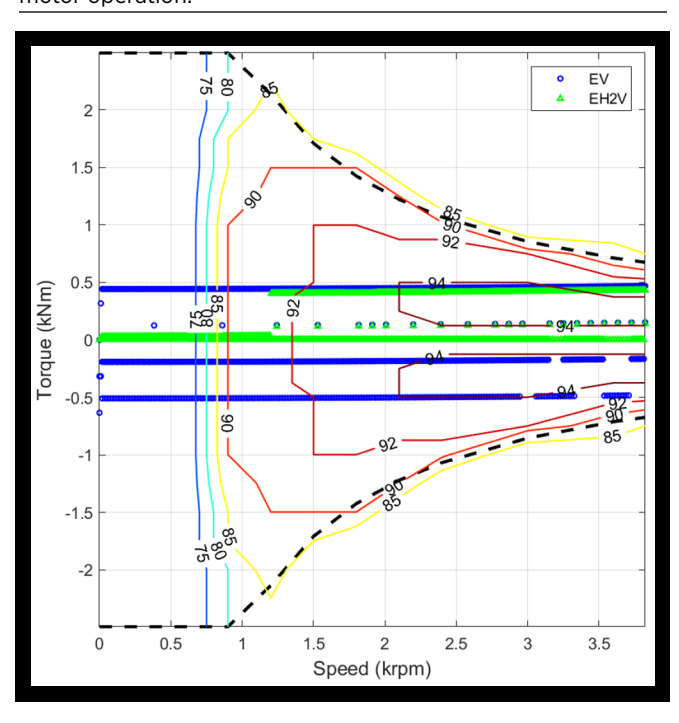
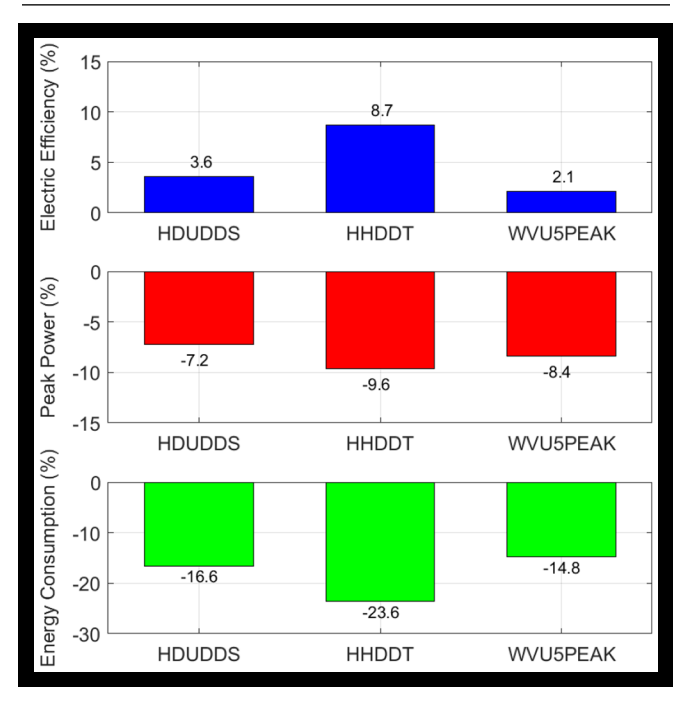


FIGURE 21 WVU5PEAK Simulation: electric motor operation.



RULE-BASED POWER MANAGEMENT STRATEGY OF ELECTRIC-HYDRAULIC HYBRID VEHICLES

FIGURE 22 Comparison: (top) total electric energy conversion efficiency; (middle) peak battery power; (bottom) total battery energy consumption.



efficiency is significantly improved by efficient operation of the electric motor and efficient hydraulic regenerative braking that stores the kinetic energy of the semi-trailer truck during deceleration and reuses it during heavy acceleration. It also turns out that the peak electric power and total electric energy consumption are significantly reduced. Such reduced electric stress offers significant benefits with respect to lower system costs by reducing the battery capacity, and longer battery service time by reducing cyclic charging and discharging the battery.

Acknowledgement

This research was supported by the National Science Foundation REU Site program under grant No. EEC-1852112.

References

- Wu, B., Lin, C.C., Filipi, Z., Peng, H., and Assanis, D., "Optimization of Power Management Strategies for a Hydraulic Hybrid Medium Truck," in *Proceedings Advanced* Vehicle Control Conference, Hiroshima, Japan, 2002.
- Kepner, R.P., "Hydraulic Power Assist A Demonstration of Hydraulic Hybrid Vehicle Regenerative Braking in a Road Vehicle Application," SAE Technical Paper <u>2002-01-3128</u>, 2002. https://doi.org/10.4271/2002-01-3128.
- 3. Baseley, S., Ehret, C., Greif, E., and Kliffken, M.G., "Hydraulic Hybrid Systems for Commercial Vehicles," SAE

- Technical Paper <u>2007-01-4150</u>, 2007. <u>https://doi.org/10.4271/2007-01-4150</u>.
- Kim, Y.J. and Filipi, Z., "Simulation Study of a Series Hydraulic Hybrid Propulsion System for a Light Truck," SAE Technical Paper <u>2007-01-4151</u>, 2007. <u>https://doi.org/10.4271/2007-01-4151</u>.
- Batavia, B.L.V., "Hydraulic Hybrid Vehicle Energy Management System," SAE Technical Paper 2009-01-2834, 2009. https://doi.org/10.4271/2009-01-2834.
- Deppen, T.O., Alleyne, A.G., Stelson, K., and Meyer, J., "A Model Predictive Control Approach for a Parallel Hydraulic Hybrid Powertrain," in *Proceedings American* Control Conference, pp. 2713-2718, San Francisco, CA, USA, 2011.
- Kim, N. and Rousseau, A., "A Comparative Study of Hydraulic Hybrid Systems for Class 6 Trucks," SAE Technical Paper 2013-01-1472, 2013. https://doi. org/10.4271/2013-01-1472.
- 8. Woon, M., Lin, Z., Ivanco, A., Moskalik, A. et al., "Energy Management Options for an Electric Vehicle with Hydraulic Regeneration Systems," SAE Technical Paper 2011-01-0868, 2011. https://doi.org/10.4271/2011-01-0868.
- 9. Lin, Z., Ivanco, A., and Filipi, Z., "Optimization of Rule-Based Control Strategy for a Hydraulic-Electric Hybrid Light Urban Vehicle Based on Dynamic Programming," *SAE Int. J. Alternative Powertrains* 1, no. 1 (2012): 249-259.
- Sun, Y., Garcia, J., and Krishnamurthy, M., "A Novel Fixed Displacement Electric-Hydraulic Hybrid (EH2) Drivetrain for City Vehicles," in *Proceedings IEEE Transportation Electrification Conference and Expo (ITEC)*, Detroit, MI, USA, June 2013.
- Chen, J.S., "Energy Efficiency Comparison between Hydraulic Hybrid and Hybrid Electric Vehicles," *Energies* 8 (2015): 4697-4723.
- 12. Leon, J., Garcia, J.M., Acero, M.J., Gonzalez, A. et al., "Cast Study of an Electric-Hydraulic Hybrid Propulsion System for a Heavy-Duty Electric Vehicle," SAE Technical Paper 2016-01-8112, 2016. https://doi.org/10.4271/2016-01-8112.
- 13. Yang, Y., Luo, C., and Li, P., "Regenerative Braking Control Strategy of Electric-Hydraulic Hybrid (EHH) Vehicle," *Energies* 10 (2017): 1038.
- 14. Niu, G., Shang, F., Krishnamurthy, M., and Garcia, J.M., "Design and Analysis of an Electric Hydraulic Hybrid Powertrain in Electric Vehicles," *IEEE T. Transportation Electrification* 3, no. 1 (2017): 48-57.
- Grzesikiewicz, W., Knap, L., Makowski, M., and Pokorski, J., "Study of the Energy Conversion Process in the Electro-Hydrostatic Drive of a Vehicle," *Energies* 11 (2018): 348.
- Hwang, H.Y., Lan, T.S., and Chen, J.S., "Optimization and Application for Hydraulic Electric Hybrid Vehicle," *Energies* 13 (2020): 322.
- 17. Ekong, U.U., Inamori, M., and Morimoto, M., "Improved Torque and Efficiency of a Four Switch Three Phase Inverter Fed Induction Motor Drive," in *Proceedings IEEE* International Conference on Power Electronics and Drive Systems (PEDS), 919-924, Honolulu, USA, 2017.

RULE-BASED POWER MANAGEMENT STRATEGY OF ELECTRIC-HYDRAULIC HYBRID VEHICLES

- 18. https://www.mathworks.com/products/powertrain.html
- 19. https://freightliner.com/trucks/ecascadia
- Corvaglia, A. and Rundo, M., "Comparison of 0D and 3D Hydraulic Models for Axial Piston Pumps," *Energy Procecia* 148 (2018): 114-121.
- 21. https://freightliner.com/trucks/ecascadia/specifications/

Contact Information

Yongsoon Yoon, Ph.D.,

Assistant Professor,

Department of Mechanical Engineering, School of Engineering and Computer Science, Oakland University, yongsoonyoon@oakland.edu

^{© 2022} SAE International. All rights reserved. No part of this publication may be reproduced, stored in a retrieval system, or transmitted, in any form or by any means, electronic, mechanical, photocopying, recording, or otherwise, without the prior written permission of SAE International.